Muon-spin-relaxation study of magnetic order in $R\mathrm{NiO_3}$ (R = rare earth) below the metal-insulator transition

J. L. García-Muñoz
Institut de Ciència de Materials de Barcelona, Consejo Superior de Investigaciones Cientificas, Campus Universidad Autónoma de Barcelona, ES-08193, Bellaterra, Spain

P. Lacorre
Laboratoire des Fluorures, U.A. CNRS 449, Université du Maine, 72017 Les Mans Cedex, France

R. Cywinski
Department of Physics and Astronomy, University of St. Andrews, North Haugh, St. Andrews, KY16 9SS, United Kingdom
(Received 7 November 1994)

Resistivity and susceptibility measurements on the perovskite $\mathrm{Nd_{0.7}La_{0.3}NiO_3}$ reveal the coincidence of magnetic and metal-insulator transitions at $T_{\mathrm{MI}}=110$ K. Muon-spin-relaxation (μSR) has been used to characterize the magnetic order in the low-temperature insulating phase. Two magnetically inequivalent muon sites exist there below T_{MI}. It is found that the crystallographically equivalent rare-earth planes split into two magnetically inequivalent planes below T_{MI}, one plane containing ordered Nd ions, the other remaining paramagnetic down to low temperatures. This behavior is a consequence of the unusual magnetic order of the Ni ions below T_{MI}, with the μSR data confirming the disappearance of the inversion center at the Ni site in the magnetic insulating regime of the $R\mathrm{NiO_3}$ perovskites.

I. INTRODUCTION

In order to understand the mechanisms responsible for superconductivity in the cuprate superconductors, it is first necessary to establish the origin of the large differences in the conductivity and the correlations between electronic and magnetic degrees of freedom in transition-metal (TM) oxides. Metal-insulator (MI) transitions are a rich source of information on the fundamental electronic energies in transition-metal oxides and afford the possibility of testing current theoretical predictions. Within the context of Coulomb correlations in the transition-metal $3d$ bands, and screening by charge transfer from the anion p bands in oxides, the discovery[1] of a thermally driven MI transition in $R\mathrm{NiO_3}$ perovskites (R = rare earth) has stimulated considerable interest: these undoped and structurally simple oxides are the only known transition-metal oxides located at the boundary that separates "low-Δ metals" from "charge-transfer (CT) insulators" in the framework developed by Zaanen, Sawatzky, and Allen[2] (ZSA). The ZSA picture accounts for the differences between metallic and insulating conductivity in a wide variety of oxides.[3]

With the exception of metallic $\mathrm{LaNiO_3}$, which has rhombohedral symmetry, these perovskite-like rare-earth nickelates are orthorhombically distorted at room temperature with the $\mathrm{GdFeO_3}$ structure (space group *Pbnm*). The MI transition temperature in $R\mathrm{NiO_3}$ decreases as the size of the rare-earth cation increases and Ni-O-Ni bond angles become straighter. No change in the symmetry of the lattice associated with the electron localization has been observed. However, we have detected a very slight expansion of the unit cell ($\Delta V/V=0.24\%$).[4] Muon-spin rotation has been used to determine the evolution of the magnetic ordering temperature with the size of the rare-earth ion,[5] showing that the magnetic transition is concomitant with the gap opening in $\mathrm{PrNiO_3}$ and $\mathrm{NdNiO_3}$, while no such correlation is found for Sm and smaller rare earths. Several features make the magnetic transition very striking. The magnetic contribution to the overall entropy change (ΔS_M) across the transition is very much lower than expected for $S=\frac{1}{2}$ Ni spins.[6] Particularly surprising is the observation by neutron diffraction of magnetic Bragg reflections well below T_{MI} in $\mathrm{PrNiO_3}$ ($T_{\mathrm{MI}}=135$ K) and $\mathrm{NdNiO_3}$ ($T_{\mathrm{MI}}=200$ K). These define a magnetic unit cell with a periodicity $(2a)\times b\times(2c)$ with respect to the crystal cell axes.[1,7,8] The observed magnetic wave vector, $\mathbf{k}=(\frac{1}{2},0,\frac{1}{2})$ in the orthorhombic cell, or $(\frac{1}{4},\frac{1}{4},\frac{1}{4})$ in the corresponding cubic subcell, defines a magnetic period in the structure that is four times the Ni-Ni distance. This situation is quite different from expected antiferromagnetically coupled $\mathrm{Ni^{III}}$ moments.

In this paper we present the results of a muon-spin-relaxation (μSR) investigation of the formation of local moments at the MI transition, and of the antiferromagnetic ground state below T_{MI}, in $\mathrm{Nd_{0.7}La_{0.3}NiO_3}$, a structurally less distorted analog of $\mathrm{NdNiO_3}$. We shall show that μSR measurements confirm that ferromagnetic and antiferromagnetic Ni couplings symmetrically coexist along the three pseudocubic axes and that there is a first-order breaking of the local symmetry at the Ni site in the *Pbnm* space group at T_{MI}. This conclusion can be drawn from the observation that the chemically identical $z=\frac{1}{4}$ and $\frac{3}{4}$ rate-earth planes split into two magnetically

dissimilar planes due to polarization by the Ni ions. The proposed magnetic order is the only solution consistent with both neutron[7,8] and muon experiments.

II. EXPERIMENT

The synthesis of the RNiO$_3$ is not straightforward, as elevated temperatures and high oxygen pressures are required. A polycrystalline sample of the solid solution $Nd_{0.7}La_{0.3}NiO_3$ was prepared from the constituent oxides under 200 bars of oxygen, as described in Refs. 1 and 5. Previous structural characterization[9] confirmed that the sample was well crystallized and single phase, with lattice parameters $a=5.4234(2)$, $b=5.3829(2)$, and $c=7.6316(4)$ Å. Resistivity, measured both on cooling and warming reveals a MI transition at 110 K, as can be seen in Fig. 1. The observed hysteresis is characteristic of a first-order transition. In Fig. 2 the susceptibility measurements indicate a magnetic anomaly also at 110 K, coinciding with T_{MI}, and a paramagnetic contribution from the Nd moments at all temperatures down to 5 K.

Zero and longitudinal field μ^+SR measurements were made on $Nd_{0.7}La_{0.3}NiO_3$ using the MuSR spectrometer at the ISIS pulsed muon facility (R.A.L., U.K.). An 11-g powder sample was mounted on an Al plate in a closed-cycle refrigerator, allowing measurements to be made over the temperature range 11–295 K. Spectra were recorded both on cooling and warming. Initially the spins of the implanted positive muons are polarized along the incident beam direction. After thermalization ($<10^{-10}$ s) they precess around local magnetic fields of both nuclear and atomic origin. If such dynamic or static fields are random, incoherent precession leads to a depolarization of the implanted muons. The decay of the muon ($\tau_\mu=2.2$ μs) is accompanied by positron emission preferentially along the muon spin direction. The resulting positron count rate, collected in time histograms in forward (F) and backward (B) detectors, therefore reflects the depolarization of the muons. The positron spectra are presented in the form of a corrected relaxation function

$$G(t)=[I_F(t)-\alpha I_B(t)]/[I_F(t)+\alpha I_B(t)]\ ,$$

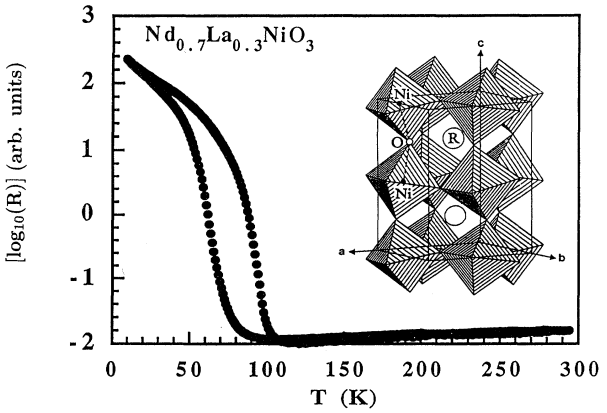

FIG. 1. The electrical resistance [$\log_{10}(R)$] as a function of temperature for $Nd_{0.7}La_{0.3}NiO_3$ measured both on cooling and warming. The crystal structure is also shown.

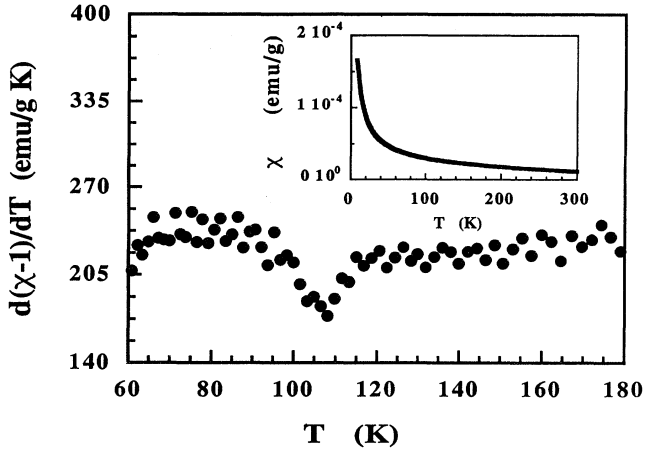

FIG. 2. The temperature dependence of the differential inverse susceptibility, $d(\chi^{-1})/dT$, for $Nd_{0.7}La_{0.3}NiO_3$ showing the magnetic anomaly coinciding with T_{MI}. The susceptibility is shown in the inset.

where I_F and I_B are the time differential positron counts in the F and B detectors. α is a calibration factor to account for the relative efficiencies of the F and B detectors: it is determined by observing the coherent muon precession in a field of 2 mT applied to the sample, transverse to the muon beam. $G(t)$ is proportional to the time-dependent muon polarization, with $G(t)=A_0P(t)$, where A_0 is the initial asymmetry, typically taking the experimental value of 0.25.

III. RESULTS AND DISCUSSION

Typical relaxation spectra, $G(t)$ from measurements of $Nd_{0.7}La_{0.3}NiO_3$ in zero field at selected temperatures (11,

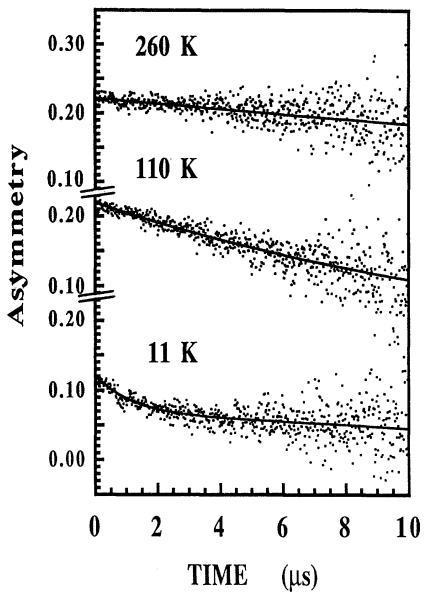

FIG. 3. The zero-field muon-spin-relaxation spectra from $Nd_{0.7}La_{0.3}NiO_3$ at 11, 110, and 260 K. The solid lines represent fits to the data using the relaxation functions discussed in the text.

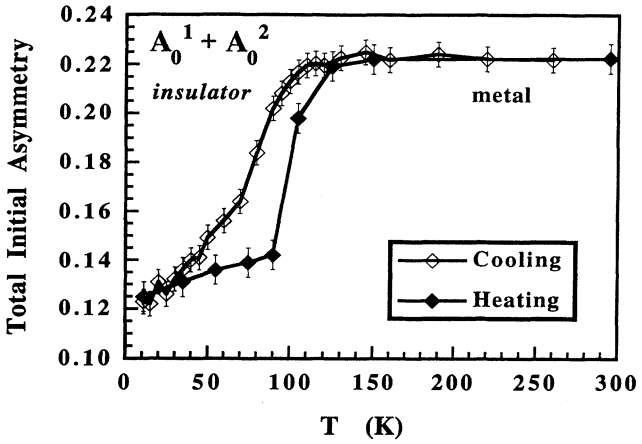

FIG. 4. Evolution of the total initial symmetry, A_0, obtained form fits of the zero-field μSR spectra from $Nd_{0.7}La_{0.3}NiO_3$ collected on both cooling and warming. Note the loss of asymmetry at T_{MI}, and the hysteretic behavior characteristic of a first-order transition.

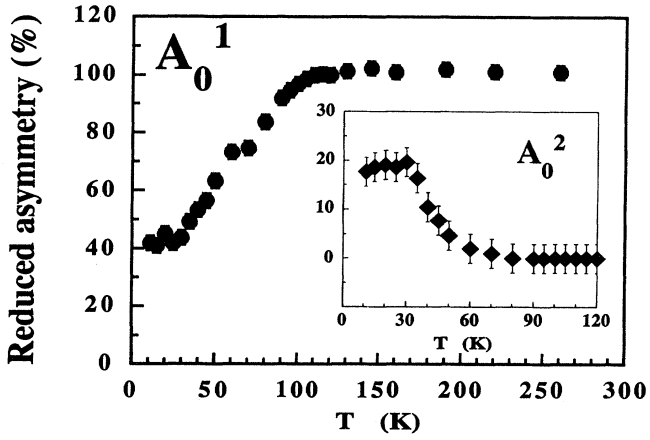

FIG. 5. Temperature dependence of the contribution to the total asymmetry A_0 of initial asymmetry parameter A_0^1 associated with $G_1(t)$. The inset shows the evolution with decreasing temperature of A_0^2, associated with the emergence below T_{MI} of a second exponential relaxation $G_2(t)$, and thus a second muon site. Both A_0^1 and A_0^2 have been normalized to the initial total asymmetry at room temperature.

110 and 260 K), are shown in Fig. 3. $G(t)$ decays monotonically with time, and no spontaneous coherent oscillations of the polarization, indicative of a unique internal magnetic field, are observed. Significant differences are found in the relaxation spectra above and below $T_{MI}=110$ K. In the metallic region ($T>110$ K) the spectra can be analyzed by adopting the functional form $G(t)=A_0\exp(-\lambda t)$. The single exponential decay indicates the presence of dynamic fields, which can be attributed to the paramagnetic spin fluctuations associated with the Nd^{3+} ions. The influence of random nuclear dipoles can be disregarded, since the observed relaxation remains unaffected by longitudinal fields of up to 0.1 T.

Below $T\approx 110$ K the asymmetry parameter A_0 begins to decrease rapidly. The thermal evolution of the asymmetry, on both cooling and heating, can be seen in Fig. 4. Marked hysteresis, again indicative of a first-order transition, is evident. The transition to the insulating, magnetically ordered, state is not only accompanied by an overall loss of asymmetry: the relaxation spectra are also modified. A satisfactory fit to the spectra below T_{MI} is only achieved by assuming a functional form composed of two independent exponential functions, with

$$G(t)=G_1(t)+G_2(t)=A_0^1\exp(-\lambda_1 t)+A_0^2\exp(-\lambda_2 t)\ .$$

The total initial asymmetry shown in Fig. 4 corresponds to $A_0=(A_0^1+A_0^2)$. In Fig. 5 we show the evolution with temperature of A_0^1 and A_0^2 individually, normalized to the room-temperature value of A_0, obtained from fits to the spectra below T_{MI}. In these oxides the magnetic phase develops very inhomogeneously, and the extremely hysteretic transition is related to the coexistence of metallic and nonmetallic phases. The thermal evolution of the respective relaxation rates λ_1 and λ_2, on both cooling and warming, are shown in Fig. 6. It should be noted that hysteresis is observed only for λ_2, which also exhibits a pronounced divergence toward low temperature. We did not observe changes of λ_1 and λ_2, within the experimental error, from longitudinal field (LF)-μSR measurements and longitudinal fields up to 0.1 T.

The marked decrease of the total initial asymmetry shown in Fig. 4 reflects the onset of static local fields below T_{MI} and can be associated with long-range magnetic order. Such order in a polycrystalline multidomain sample might be expected to lead to a coherent muon precession arising from the two transverse field components together with a nonprecessing contribution resulting from the longitudinal field component: the asymmetries associated with the precessing and nonprecessing components are distributed in the ratio $\frac{2}{3}:\frac{1}{3}$, respectively. However, the finite pulse width (70 ns) of the muon beam

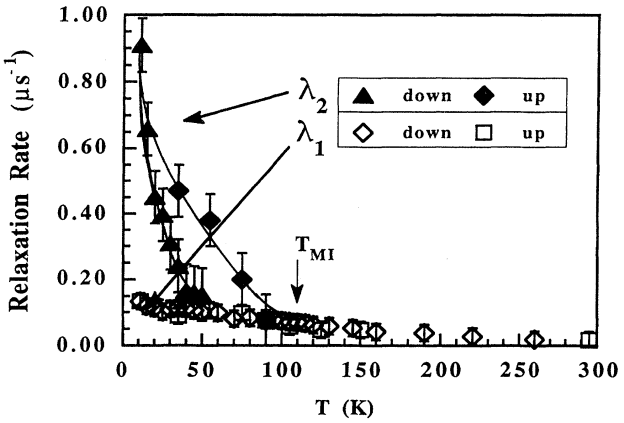

FIG. 6. Thermal evolution of the exponential damping rates λ_1 and λ_2. At $T_{MI}=110$ K, λ_1 evolves smoothly into the single relaxation rate λ observed at higher temperatures. (Solid lines are guide lines.)

at ISIS restricts the frequency response of MuSr:[10] a unique internal transverse field much greater than approximately 50 mT results in a coherent precession beyond the effective frequency window of the instrument and therefore in a loss of initial asymmetry. The Ni-O subsystem in these nickelates is Pauli paramagnetic in the metallic state above T_{MI}.[8,11] The loss of asymmetry at T_{MI}, and its coincidence with the anomaly in $\chi(T)$, seen in Fig. 2, must therefore be attributed to the formation of local moments at the Ni sites, and the ensuing long-range magnetic order. However, it should be noted that only 35% of the initial asymmetry is lost, rather than the predicted $\frac{2}{3}$. This, together with the observation of two exponential relaxation functions below T_{MI} indicates that there are two muon sites in RNiO$_3$, one sensing essentially static local fields (associated with magnetic order) and the second sensing fluctuating fields. To understand the implications of this result, we now need to review the analysis of the neutron-powder-diffraction measurements on the RNiO$_3$ compounds.

Two magnetic structures were found to be consistent with the observed neutron-powder-diffraction patterns from PrNiO$_3$ and NdNiO$_3$,[8] well below the metal-insulator transition ($T<20$ K). In the first model (model 1 in Fig. 7) each Ni^{III} ($S=\frac{1}{2}$, $\mu_{Ni}=0.9\mu_B$) is coupled ferromagnetically (F) to three Ni nearest neighbors and antiferromagnetically (AF) coupled to the remaining three neighbors through the oxygen ions at the vertices of the NiO$_6$ octahedra (Fig. 7). This is achieved by a symmetrical arrangement of F and AF coupled pairs of Ni-O-Ni units (i.e., Ni↑-O-Ni↑-O-Ni↓) related by the inversion center at the Ni site in the *Pbnm* space group. The rare-earth sites are bracketed by planes of Ni octahedra and, in this model, the ordering of the Ni moments results in the single crystallographic Nd site splitting, at low temperatures, into two magnetically inequivalent sites: the rare-earth plane at $z=1/4$ is polarized by the Ni moments, and magnetically orders at low temperatures ($\mu_{Nd_1}=\mu_{Nd_4}=2.2\mu_B$), while there is a nulled exchange field at the $z=\frac{3}{4}$ plane, and the Nd ions remain disordered ($\mu_{Nd_2}=\mu_{Nd_3}=0$) down to the lowest temperatures (see Fig. 7). In the second solution (model 2, Fig.7), all rare-earth sites have identical ordered moments, while Ni$_1$ and Ni$_3$ sites are ordered with $\mu_{Ni}=1.8\mu_B$ (Ni^{2+}, high spin) with the remaining Ni atoms adopting the diamagnetic Ni^{2+} state. The agreement factors for these two models are identical for the neutron diffraction pattern from PrNiO$_3$, and somewhat more satisfactory for model 1 in the case of NdNiO$_3$.

Considering now the muon localization site in the RNiO$_3$ compounds, we note that information can be inferred from previous measurements on the orthoferrites, RFeO$_3$, which are isostructural with RNiO$_3$. In the orthoferrites the muon site has been established unambiguously and without *a priori* assumptions.[12] If we assume here that as in the orthoferrites $(O\mu)^-$ bonds are formed, the muon site should be determined by the approximately 1-Å $+\mu$-O^{2-} bond length and by Coulomb interactions with the neighboring atoms. We are thus led to conclude that the muons in RNiO$_3$ localize on the mirror plane m on the rare-earth layer, approximately 1 Å from the nearest oxygen ion, very close to the interstitial site determined for RFeO$_3$,[12] i.e., at $(x,y,\frac{1}{4})$ with $x=0.98$, $y=0.58$. This implies an O-μ distance of 0.71 Å in the nickelates. The location of the muons at the $z=\frac{1}{4}$ and $\frac{3}{4}$ planes is illustrated in the RNiO$_3$ structure in Fig. 7. The interstitial muon site is thus located almost at the center of the slightly distorted square formed by the nearest-neighbor rare-earth ions. For our Nd$_{0.7}$La$_{0.3}$NiO$_3$ sample the $^+\mu$-Ni distance is $c/4=1.91$ Å and the $^+\mu$-R distance is $a/2=b/2=2.7$ Å.

Clearly the low-temperature magnetic environment of this muon site is very different for models 1 and 2 discussed above (Fig. 7). For model 2 there is a single magnetic environment, with all the in-plane R ions magnetically ordered and only one of the two out-of-plane Ni atoms possessing an ordered moment. For model 1, on

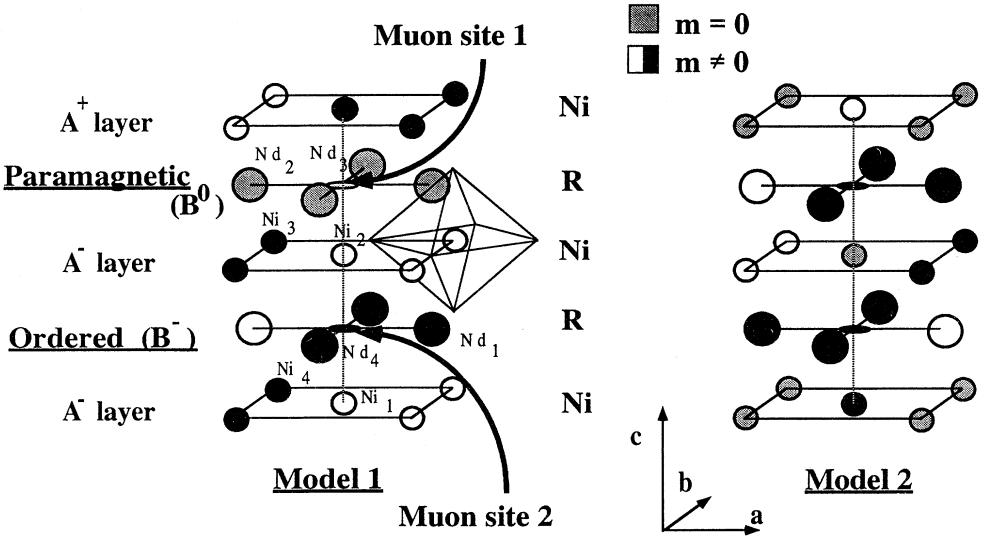

FIG. 7. The two magnetic models, model 1 and model 2, suggested by neutron diffraction from NdNiO$_3$ and PrNiO$_3$ at low temperatures. Note the different effective fields acting on the rare earth $z-\frac{1}{4}$ and $\frac{3}{4}$ planes in model 1. The position of the muon localization site in the structure, inferred from μSR studies of the isostructural orthoferrites RFEO$_3$ is also shown.

the other hand, two distinct magnetic muon environments are evident: the muon can be located on the $B^{\pm}$ plane (between $A^{\pm}$-$A^{\pm}$ ordered Ni layers) with a nonzero internal field at the R^{3+} sites, and on the B^0 plane (between $A^{\pm}$-$A^{\mp}$ Ni layers) for which the internal field at the R^{3+} is null.

We can see that only model 1 can provide a framework within which the μSR results, which indicate two independent magnetic environments, can be understood. The muons located at the B^0 plane are not sensitive to the onset of long-range magnetic order of the Ni ions at T_{MI}. Instead they see only the fluctuating magnetic fields resulting from the paramagnetic R^{3+} spins on the B^0 plane. The dynamic relaxation component $G_1(t)=A_0^1\exp(-\lambda_1 t)$ can be associated with these muons: in Fig. 6 it can be seen that the relaxation rate λ_1 evolves smoothly through T_{MI} into λ determined from analysis of the relaxation spectra above T_{MI}. However, the muons on the $B^{\pm}$ plane sense a significant effective field from ordered Ni moments below T_{MI}. This leads to the loss of $\frac{2}{3}$ of the asymmetry associated with this site, due to muons precessing in the transverse internal field components. The relaxation function $G_2(t)=A_0^2\exp(-\lambda_2 t)$, hence, represents the remaining $\frac{1}{3}$ of muons at the $B^{\pm}$ planes, which sense only the polarizing longitudinal internal field components. The exponential form of $G_2(t)$ indicates the presence of residual fluctuating fields at the $B^{\pm}$ planes. Indeed the relaxation rate λ_2 exhibits a marked and hysteretic divergence toward low temperatures. We attribute this divergence to a slowing down of the paramagnetic Nd^{3+} spins on the $B^{\pm}$ planes as these spins polarize in the exchange field of the Ni ions. In pure $NdNiO_3$ this polarization is observed below 15 K. At the lowest temperatures, and considering the estimated error, $\approx 43\pm 3$ % of all muons are at site 1 and about $55-8$% at site 2. These numbers are very close to 50%, and in their determination muons have been considered motionless, fixed at one of the two sites. A certain spread of the dynamic field at the muon sites is also probable due to the presence of nonmagnetic La ions homogeneously distributed at the rare-earth site in the sample.

To our knowledge, these μSR results represent the first experimental evidence, independent of neutron diffraction, which can confirm that the $RNiO_3$ perovskites, with R=Nd,Pr, order with the magnetic structure designated "model 1" in Ref. 8. In Fig. 8 we present the thermal evolution of ordered Nd moments in the parent compound $NdNiO_3$ ($T_{MI}=200$ K) obtained by analyzing the neutron-diffraction data from this compound within the framework of this model. In the present $Nd_{0.7}La_{0.3}NiO_3$ sample, the Nd ions will, of course, order at a lower temperature.

The unusual magnetic order associated with the Ni sublattice has important implications, since the nature and sign of the exchange interactions are associated with the orbital occupancy of the e_g^1 electrons of the Ni^{III} ions (d^7:$t_{2g}^6 e_g^1$). According to the Hund-Kanamori rule the magnetic structure of $Ni^{III}(t_{2g}^6 e_g^1)$ clearly suggests a ground state in which e_g electrons break up into two sublattices, each with one of the $d_{3z^2-r^2}$ or $d_{x^2-y^2}$ orbitals half occupied. Neighboring Ni atoms with electrons in the same orbital will be antiferromagnetically coupled, and those occupying different orbitals will align with spins parallel. The stability of such orbital ordering could be disrupted by the closing of the gap. The nonuniform orbital distribution of the single e_g electron may result from the breakdown of the degeneracy of the Ni^{III} state.

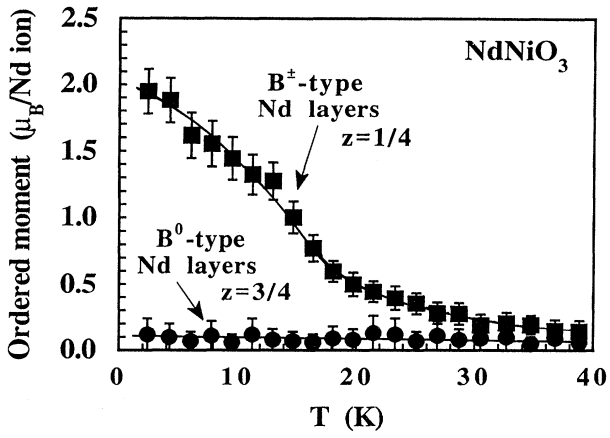

FIG. 8. The evolution with temperature of the average Nd moments in $NdNiO_3$ ($T_{MI}=200$ K) obtained by analyzing previous neutron-diffraction data using model 1 discussed in the text. Those Nd ions on the $z=\frac{1}{4}$ plane in Fig. 7 are polarized, while those in the $z=\frac{3}{4}$ plane remain paramagnetic at all temperatures.

In summary, the muon-spin-relaxation spectra of $Nd_{0.7}La_{0.3}NiO_3$ provide clear evidence that below the metal-insulator transition at $T_{MI}=110$ K there exist two magnetically inequivalent muon sites. At one of the sites the muons sense, simultaneously, the long-range magnetic order of the Ni sublattice, together with a slowing of spin fluctuations associated with the increasing polarization of in-plane ($z=\frac{1}{4}$) Nd moments. In the $z=\frac{3}{4}$ plane the unusual magnetic order of the Ni planes results in a cancellation of the internal magnetic field at both the second muon site and the Nd site. As a result the muons at this site sense only the spin fluctuations associated with nonpolarized Nd moments. These results, together with previous neutron-diffraction measurements, have enabled us to establish unambiguously the arrangement of spins in these $RNiO_3$ preovskites. The resulting spin structure, which implies the disappearance of the inversion center at the Ni site in the *Pbnm* space group, has not been observed in other perovskite oxides. Whether the symmetrical coexistence of ferromagnetic and antiferromagnetic coupling is a consequence of an orbital superlattice of the Ni e_g electron due to electronic correlations deserves further investigation.

ACKNOWLEDGMENTS

The μSR measurements at ISIS were supported by the EC Large Installation Plan of the Human Capital and Mobility Programme. The authors would like to thank S. H. Kilcoyne for experimental support on MuSR, X. Granados for the resistivity measurements, and J. Rodríguez-Carvajal for fruitful discussions. A. I. Nazzal and J. B. Torrance are gratefully acknowledged for supplying the sample. J.-L.G.-M. would like to acknowledge the CSIC-CIRIT and the Spanish DGICYT (Grant No. PB92-0849) for financial support, and R.C. acknowledges financial support from the EPSRC.

[1]P. Lacorre, J. B. Torrance, J. Pannetier, A. I. Nazzal, P. W. Wang, T. C. Huang, and R. L. Siemens, J. Solid State Chem. **91**, 225 (1991).

[2]J. Zaanen, G. A. Sawatzky, and J. W. Allen, Phys. Rev. Lett. **55**, 418 (1985).

[3]J. B. Torrance, P. Lacorre, C. Asavaroengchai, and R. M. Metzger, J. Solid State Chem. **90**, 168 (1991).

[4]J. L. García-Muñoz, J. Rodríguez-Carvajal, P. Lacorre, and J. B. Torrance, Phys. Rev. B **46**, 4414 (1992).

[5]J. B. Torrance, P. Lacorre, A. I. Nazzal, E. J. Ansaldo, and Ch. Niedermayer, Phys. Rev. B **45**, 8209 (1992).

[6]X. Granados, J. Fontcuberta, X. Obradors, Ll. Mañosa, and J. B. Torrance, Phys. Rev. B **48**, 1166 (1993); J. L. García-Muñoz *et al.* (unpublished).

[7]J. L. García-Muñoz, J. Rodríguez-Carvajal, and P. Lacorre, Europhys. Lett. **20**, 241 (1992).

[8]J. L. García-Muñoz, J. Rodríguez-Carvajal, and P. Lacorre, Phys. Rev. B **50**, 978 (1994).

[9]M. Medarde, J. L. García-Muñoz, S. Rosenkranz, X. Granados, J. Fontcuberta, and P. Lacorre, Physica B **194-196**, 367 (1994); G. H. Eaton, Z. Phys. C **56**, S232 (1992).

[10]A. Schenck, *Muon Spin Rotation Spectroscopy: Principles and Applications in Solid State Physics* (Adam-Hilger, Bristol, 1985), p. 27.

[11]J. B. Goodenough, N. F. Mott, M. Pouchard, G. Demazeau, and P. Hagenmuller, Mater. Res. Bull. **8**, 647 (1973).

[12]E. Holzschuh, A. B. Denison, W. Kündig, R. F. Meier, and B. D. Patterson, Phys. Rev. B **27**, 5294 (1983).